Iron removal from raw asbestos by siderophores-producing Pseudomonas

Sébastien R. David, Dris Ihiawakrim, Robert Regis, Valérie A. Geoffroy

Iron removal from raw asbestos by siderophores-producing *Pseudomonas*

Sébastien R. David [a,b], Dris Ihiawakrim [c], Robert Regis [d], Valérie A. Geoffroy [a]

[a] Université de Strasbourg, CNRS-UMR7242, BSC, ESBS, 300 Bld Sébastien Brant, 67413 Illkirch, Strasbourg, France
[b] Agence de l'Environnement et de la Maîtrise de l'Energie, 20 avenue du Grésillé, BP 90406, 49004 Angers Cedex 01, France
[c] Université de Strasbourg, CNRS-UMR7504, IPCM, 23 rue du Loess, BP 43, 67034 Strasbourg, France
[d] SOMEZ, Parc Marcel Dassault, 470 Rue Alberto Santos Dumont, 34430 Saint Jean de Vedas, France

To whom correspondence should be addressed: V. A. Geoffroy, UMR 7242, Université de Strasbourg-CNRS, ESBS, Biotechnologie et Signalisation Cellulaire, Bd Brant, CS 10413, F-67412 Illkirch Cedex France.
Email : valerie.geoffroy@unistra.fr
Tel. (+33) 3 68 85 47 51
Fax (+33) 3 68 85 48 29

Abstract

Asbestos, mineral present in soil, are highly toxic due to the presence of iron. Microbes-mineral interactions occur naturally through various processes leading to their alteration. We examined the effect of siderophore-producing *Pseudomonas* with a particular focus on the role of pyoverdine and pyochelin on raw asbestos fibers such as amosite, crocidolite and chrysotile. We compared the efficiency of pyoverdine to the iron chelating agent EDTA in the release of iron from raw asbestos fibers. Pyoverdine was able to extract iron from all the tested raw asbestos with the higher efficiency observed for chrysotile and crocidolite. When asbestos were grinded, the iron removal was more important for all types. We monitored the effect of bacterial growth and siderophores containing bacterial supernatant on raw asbestos dissolution by solution chemistry analysis and transmission electron microscopy. The siderophore-containing supernatant allowed a higher iron solubilisation than the one obtained after bacterial growth. Moreover, the iron dissolution was faster with pyoverdine-containing supernatant than pyochelin-containing supernatant, with approximately the same iron level for the maximum extraction with a delay of 48 h. Our study clearly showed the involvement of bacterial siderophores, pyoverdine and pyochelin on chrysotile, crocidolite and amosite fibers weathering.

Keywords

Iron-Asbestos-Weathering- Siderophore-*Pseudomonas*

1. Introduction

Asbestos has been extensively used for building constructions during the industrial exploitation in 1900's before it was banned in 1997 in France. The management of huge amount of wastes is a major concern today since asbestos-containing wastes represent an environmental and health problem. Asbestos fibers inhalation leads to various types of toxic effects in human such as inflammation and fibrogenesis of lung, mesothelioma or bronchogenic carcinoma. Asbestos are natural fibrous silicates belonging to serpentine and amphibole families. Chrysotile, the only member of the asbestiform serpentine is widely present among wastes (90-95%), while amphibole can be found in a minor extent compared to chrysotile in wastes. Among these, crocidolite and amosite are the two members of the amphibole, which have been found among the greatest commercial applications. The crystalline structures of fibers of amphiboles and serpentine are well described [1,2] and it explains the opposite chemical susceptibility towards acids or bases, e.g. chrysotile fibers are easily attacked by acidic condition while amphibole are in basic solution. The chrysotile structure is composed of a double layer consisting of a tetrahedral (silicate) sheet and a magnesium hydroxide octahedral sheet (brucite). This theoretical structure can vary if Fe^{2+} substitutes with Mg^{2+} in the brucite sheet. Up to 5% iron can be encountered in fibers since it is a relatively abundant element in many soils where asbestos natural rocks are originated. A double-tetrahedral silicate chain characterized the amphibole crystalline structure combined with a layer composed of ions mostly Mg^{2+}, Ca^{2+}, Na^{+}, Fe^{2+}, or Fe^{3+} (Table 1). Asbestos toxicity is correlated to the presence of iron as a catalyst of the Fenton reaction leading to the generation of free radicals and reactive oxygen species (ROS) [3,4].

Iron is an essential nutrient for most living organism to sustain their growth, although it is mostly unavailable in the environment. Iron is naturally abundant in soil, where it can be found in iron-bearing minerals such as goethite or ferrihydrite as iron oxides or clays for example. Therefore, many strategies have been developed by organisms such as fungi, plants or bacteria to have access to this element essential for their growth. Siderophore production, small molecules with a high affinity for Fe(III) produced in iron limited conditions, has been

described as one the common weathering process for fungi, plants and bacteria in various interactions with minerals [5]. For example, the dissolution of goethite mediated by the fungus *Suillus granulatus* [6] or various iron oxides solubilized by the phytosiderophore mugineic acid has been reported [7]. Kalinowski *et al*. [8] and Rosenberg and Maurice [9] reported hornblende and kaolinite dissolution rates depending on desferrioxamine-B, a bacterial siderophore that enhanced iron solubilisation. Asbestos, as a fibrous silicate mineral, is no exception to natural weathering by biological processes. Few studies investigated the biological alteration of raw asbestos. Indeed, telluric bacteria such as *Bacillus mucilaginosus* induced a mineral dissolution with an interestingly loss of crystallinity in the serpentine fibers along with a pH decrease, organic acids and ligand secretion [10]. Other bacteria isolated from asbestos rocks or soil from several indian mines, without species identification, decreased the iron content of asbestos rocks [11]. Further studies on these mine-isolated bacteria showed the production of siderophore which could be involved in the weathering process, however with no evidence on the structure of the produced siderophores [12]. Moreover, Rajkumar *et al*. [13] described the plant growth-promoting mechanisms involving siderophore-producing-bacteria in a serpentine soil where siderophore is one of the various strategies to remove nutrient elements essential for plant growth. Few siderophores demonstrated their ability to release iron from asbestos fibers. Indeed, iron removal by desferrioxamine siderophore evidenced from raw asbestos, on chrysotile fibers [14] and amphibole fibers such as crocidolite and amosite [15]. Siderophore-producing *Pseudomonas* are widespread bacteria in soil and known for mineral-weathering capacity. The genus *Pseudomonas* produces a wide variety of siderophores and more than 98 % of different fluorescent *Pseudomonas* isolated from soil, produce detectable siderophore under iron starvation [16]. The range of siderophore concentrations found in soil is wide, from tens of micromoles to a few millimoles per litre [17]. *Pseudomonas aeruginosa* is an ubiquitous fluorescent *Pseudomonas* found in various environment [18], whose siderophore production and iron acquisition are well known [19]. *P. aeruginosa* produces two endogenous siderophores, a more energy demanding high affinity molecule, pyoverdine (PVD) [20] and a low affinity siderophore, pyochelin (PCH) [21]. Pyoverdine is composed of three distinct structural parts i) a dihydroxyquinoline chromophore which confers the color and the fluorescence of the molecule ii) a peptide chain comprising 6 to 12 amino acids bound to its

carboxyl group iii) a small dicarboxylic acid (or its monoamide) connected amidically to the NH_2-group [22–26]. Pyoverdine chelates iron with a Ka of $10^{32}M^{-1}$ and in 1:1 stoichiometric ratio, via the catechol group of the chromophore and the two hydroxyornithines of the peptide moiety [27]. The structure of pyochelin is a derivative of a salicylic acid, which chelates iron with an affinity of $10^{28.8}M^{-2}$ [28] and a 2:1 (PCH : Fe^{3+}) stoichiometry : a tetra-dentate is provided by one molecule of PCH and a bi-dentate by the second PCH to complete the hexacoordinate octahedral geometry necessary for iron chelation [29]. Some studies were shown the ability of siderophore-producing *Pseudomonas* to interact with minerals. For example, *Pseudomonas mendocina* dissolved hematite or goethite, iron oxides, by iron mobilization from these minerals by bacterial metabolism [30]. Moreover, Ferret *et al*. [31] showed the ability of *P. aeruginosa* to solubilize structural iron from smectite, involving the pyoverdine and pyochelin in release process. Smectite is, a type of clay with silicate sheet structure, which structure share a common feature with asbestos minerals.

The aim of the present study was to investigate the bioweathering process of chrysotile or amphibole type by siderophore-producing *Pseudomonas*. Therefore, we compared the efficiency of pyoverdine to the chemically iron chelator, Ethylenediaminetetraacetic acid (EDTA), in the release of iron from raw asbestos. We examined the role of the *P. aeruginosa* siderophores, the pyoverdine and pyochelin in the asbestos alteration. This work provide a better understanding of the bacterial interaction with asbestos to further develop in the future a bioremediation process based on bacterial and/or siderophore alteration.

2. Experimental

2.1. Raw asbestos preparation

Three types of raw asbestos were used (chrysotile (CHR), crocidolite (CRO) and amosite (AMO), table 1) with or without manual grinding. All asbestos samples (0.125 g) were immersed in distilled water and sterilized by autoclave (121°C for 20 min). Samples were then incubated at 70°C for 14 days before experiments for a complete sterilization of materials. The heat removed any water allowing to weight samples with precision.

2.2. Pyoverdine purification

P. aeruginosa ATCC 15692 was grown in Luria Bertani medium (LB) for 15 h at 30°C under shaking condition (220 rpm). 1 mL of LB culture was centrifuged (3 min at 9871 g). To obtain iron starved cells, the iron-deficient succinate medium (composition in g L^{-1}: K_2HPO_4, 6.0; KH_2PO_4, 3.0; $(NH_4)_2SO_4$, 1.0; $MgSO_4.7H_2O$, 0.2; sodium succinate, 4.0; pH adjusted to 7.0 by addition of NaOH), sterilized by 0.2 µm filtration, was used [20]. The pellet, washed twice with 1 ml of succinate medium, was suspended in 1 ml of succinate medium and inoculated in 15 mL of sterile succinate medium, incubated at 30°C under shaking condition (220 rpm). After 24 h of growth, 7.5 mL of this culture was transferred in an Erlenmeyer flask containing 1 L of succinate medium. After 24 h of incubation, the culture was centrifuged (2664 g for 40 min). Then, the supernatant was filtered twice with Whatman filter and once on nitrocellulose filter (0.45 µm porosity). Siderophore containing supernatant was loaded, after acidification (pH 6.0), on XAD-4 column, washed with two volume of purified water and eluted with one volume of 50% ethanol. The green fraction was concentrated under vacuum on a rotary evaporator and lyophilized.

2.3. Bacterial strains and growth conditions

We used the wild-type *P. aeruginosa* ATCC 15692 strain and two siderophore mutants, PAO6297, a pyochelin-deficient strain (ΔPCH) [32] and PAO6382, a pyoverdine-deficient strain (ΔPVD) [33] (Table 2). Bacteria were grown at 30°C overnight in LB broth medium at 200 rpm. For iron-depleted culture, cells were harvested from a LB pre-culture (24 h incubation), washed twice in succinate medium and used to inoculate fresh succinate medium. The cultures were incubated for 24 h under shaking (200 rpm). A second transfer in succinate medium was done in the same condition. After 24 h, the culture was centrifuged (10 min at 9871 g) and the pyoverdine-containing supernatants were sterilized by filtration (0.22 µm porosity). To prepare the bacterial suspension, cells were washed twice with sterile succinate medium. Bacterial cell density was adjusted to OD_{600} at 0.05 corresponding to 1-4 x 10^7 CFU/ml.

2.4. Dissolution of iron from asbestos fibers

Dissolution of iron from asbestos fibers by EDTA or purified pyoverdine produced by *Pseudomonas aeruginosa* ATCC 15692 was compared. Both chelators were prepared in succinate media at a final concentration of 200 µM. Asbestos samples of CHR, CRO and AMO, grounded manually or not, were spiked into 20 mL of each chelator. Assays were incubated at 30°C under shaking condition (220 rpm) during 48 h. After this first cycle

contact, the assays were centrifuged 30 min at 9871 g to recover supernatants. In order to continue alteration, two others cycles were repeated during 48 h and 96 h in the same conditions. Each assay was done in triplicate and the results are the mean of triplicate.

Dissolution of iron from asbestos fibers by bacteria or bacterial supernatants was done at 30°C under shaking conditions (220 rpm) with the 3 types of grinded asbestos. Pyoverdine-containing supernatant and bacterial cell suspension were prepared as described on paragraph 2.3. After a first cycle of 48 h alteration, assays were centrifuged 30 min at 9871 g. For each renewal, 20 ml of siderophore-containing supernatant or a bacterial suspension of OD_{600} at 0.05 were added to respective samples. Renewal cycles of 48 h were performed twice for both conditions. Every 48 h cycle, bacterial number was determined by serially diluted and plated on LB plates incubated at 30°C for 24 h. All supernatants were sterilized by filtration (0.22 µm porosity). Each assay was done in triplicate and the results are the mean of triplicate. Samples of raw crocidolite incubated with bacteria and its abiotic control were observed by transmission electron microscopy at the end of the experimental cycles.

In order to determine iron content in supernatant, solutions were acidified to 1% with nitric acid and iron was determined by atomic absorption spectroscopy (Perkin-Elmer AAnalyst 400).

2.7. STEM-EDX of asbestos fibers

TEM (Transmission Electron Microscopy) images were recorded with a JEOL 2100 microscope, with a 200 kV potential applied on a LaB6 filament as an electron source. Resolution of the TEM is 0.21 nm. TEM mapping was performed in STEM (Scanning transmission electron microscopy) mode (resolution 2 nm) and using an SSD-EDX (Silicon Drift Detector-Energy Dispersive X-ray) spectrometer to determine the chemical composition.

2.8. Statistical analysis

Differences of iron concentrations after pyoverdine and EDTA treatments solubilized from asbestos fibers were determined using Kruskal-Wallis test (RStudio v1.0.153) followed by a Conover post-hoc analysis.

Results and discussion

1.1. Comparison of pyoverdine and EDTA treatments

For the three asbestos, chrysotile, crocidolite and amosite, iron was released in the presence of the iron-complexing agents, pyoverdine or EDTA at each renewal cycle. Whichever the asbestos family, serpentine (chrysotile) or amphiboles (Amosite, Crocidolite), the iron release was possible even if the crystalline structure was very different (Fig. 1). Our result showed that the bacterial siderophore pyoverdine produced by fluorescent *Pseudomonas* was able to remove iron from asbestos fibers. During the three incubation period, the bacterial siderophore pyoverdine extracted more iron than the chemical chelator EDTA for chrysotile (0.38 to 1.04 mg/L and 0.08 to 0.19 mg/L respectively) (Fig. 1A-B) and crocidolite (0.59 to 3.84 mg/L and 0.12 to 1.92 mg/L respectively) (Fig. 1C-D). Unlike the last two asbestos, pyoverdine and EDTA revealed the same efficiency towards amosite fibers (1.07 to 3.58 and 0.82 to 3.64 mg/L respectively) (Fig. 1E-F). Differences between pyoverdine and EDTA efficiency may be explain by their affinity and specificity for iron. Indeed, pyoverdine chelates iron with an affinity of 10^{32} M^{-1} while EDTA has a lower Ka of 10^{20} M^{-1} [34]. When asbestos were grinded, iron weathering increased in the presence of EDTA or pyoverdine with an efficiency ranging from 1.3 times and 2 times for chrysotile and amosite respectively and 2 to 5 times for crocidolite (Fig. 1). Grinding lead to the amorphization of chrysotile with probably the direct OH bonds between the silica and brucite sheets destroyed or opened [35]. Moreover, grinding may also increase the exchange surface capacity between pyoverdines and asbestos, improving the extraction and accessibility of iron release. Similar results were obtained by Chao *et al*. [15] where EDTA or citrate were also able to extract iron from crocidolite or amosite but to a lesser extent that the bacterial siderophore desferrioxamine. Werner *et al.* [36] observed the same findings on crocidolite under 30 days of contact with the ranking desferrioxamine > EDTA > citrate. Ferrozine, an iron(II) chelator, was able to extract iron from crocidolite and amosite, while the iron extraction from chrysotile was only possible when ascorbic acid was supplemented [14]. Recently, Desferrioxamine and ferrichrome extracted iron for raw chrysotile at the same level but with no synergy when organic acids were supplemented or tested alone [37].

1.2. Dissolution of iron by siderophore-producing bacteria

We have shown that pyoverdine was able to withdraw iron from the three commonly found raw asbestos fibers. Since asbestos were extracted from soils, like numerous telluric microorganisms such as fluorescent *Pseudomonas*, we wanted to evaluate the role of *P. aeruginosa* compared to potential metabolites produced during an iron-starved culture in the release of iron. Therefore, asbestos samples were incubated with cells or bacterial supernatant of *Pseudomonas* producing only pyoverdine, only pyochelin or producing both endogenous siderophores. Removal of iron was measured after three successive contact cycles of 48 h. The amount of iron released in the presence of bacterial supernatants at any given cycle was higher than in the presence of bacterial cells for chrysotile and crocidolite (Fig. 2A, B, C, D). During the first 48 h contact cycle (T48) with chrysotile (Fig 2A), a rapid release of iron was observed for the wild-type and the ΔPch pyoverdine-containing supernatant, which dissolve iron 2 to 3 times more efficiently than the ΔPvd supernatant, producing only pyochelin. For the second cycle (T48-2), results are reversed since the ΔPvd supernatant extracted twice as much iron than the WT and ΔPch supernatant for chrysotile, results are also valid for crocidolite. Interestingly, for chrysotile and crocidolite, pyochelin containing supernatant at T48-2 cycle extracted the same iron amount than the pyoverdine containing supernatant at T48 but required twice as much time. For the last cycle (T48-3), the same tendency is noticed for chrysotile between the 3 supernatants but to a lesser extent than the T48-2. For crocidolite in the T48-3 cycle, the maximum iron content (0.78 mg/L) was observed for the WT supernatant compared to previous cycles (0.41 and 0.34 mg/L for T48 and T48-2). For amosite, a very low efficiency for all the supernatants was noticed between 0.04 and 0.17 mg/L. In the presence of bacteria, only the ΔPch strain (0.28 mg/L) seemed to be more effective in iron removal at the T48-3 cycle. No changes were observed in culture medium alone or culture medium containing either fibers or bacteria (Fig. 2.). Our results showed that iron dissolution is more rapid and important for chrysotile compared to amphibole. Such differences can be explained by crystal structure of asbestos and the iron-binding sites [38]. Indeed, in the chrysotile structure the octahedral layer (brucite) magnesium can be substituted by iron while in the tetrahedral layer, silicon may be rarely replaced by iron. In amphibole structure, iron is bound in cationic sites present in two ribbons of silicate tetrahedra. Therefore, iron is more easily available in chrysotile (brucite outer layer) compared to amphibole whose iron is trapped in two silicate layers.

Together with these high affinity iron chelators produced in the supernatant, physiological organic acids could be also encountered during bacterial growth, which may have a

synergistic effect in iron release [39]. Another described parameter is the grinding which enhanced iron dissolution [40,41]. In our study, considering that all asbestos fibers were manually grinded, this parameter could have influenced the iron solubilisation, since it was difficult to obtain homogeneous grinding samples between experiments. As a consequence, lower iron concentrations were observed for supernatant-treated crocidolite and amosite compared to the purified pyoverdine treatment. It is well known that siderophore-mediated iron removal involve siderophore adsorption on the iron-bearing mineral surface [5]. Therefore, the grinding may increase the specific surface area of asbestos and improve accessibility of siderophores to iron on the surface. Moreover, the presence of organic acids in the supernatant could have influenced the chrysotile dissolution since the amount of dissolved iron at 48 h (2.54 mg/L) in the supernatant is higher compared to the purified pyoverdine dissolution test (0.83 mg/L, Fig. 1B). At the second renewal, the same influence was noticed with values three times higher for the supernatant (Fig. 2A) compared to the purified pyoverdine (Fig. 1B). Differences could not be due to (i) pyoverdine degradation since this molecule has been shown to be stable in those conditions (ii) pyoverdine concentration since it was tested at the same level between the purified and the one synthesized by cells after 48 h.

Our results confirm that *Pseudomonas* was able to promote mineral dissolution concomitantly with siderophore production. Compared with data related to asbestos-fungi alteration, few researches were focused on asbestos-bacterial interactions. As an example of Gram-positive bacteria, *Bacillus mucilaginosus* was able to accelerate serpentine powder thanks to organic acids and ligands [10]. Bhattacharya *et al.* [11] isolated Gram positive and Gram negative bacteria from Indian asbestos contaminated soil or asbestos rocks which induced a decrease in the iron content of asbestos after bacterial weathering. Further research, focused on the Gram positive previously isolated strains, revealed the production of siderophores from these bacteria, with no precise identification of the produced compounds [12]. Bacterial siderophores produced by *Staphylococcus* mines isolates [11,12] were also implicated in iron removal from asbestos rocks, together with desferrioxamine from crocidolite fibers [42]. This strategy to overcome iron limitation is also well documented for soil organisms since several fungi have been reported to be involved in iron sequestration [43]. Bioweathering abilities of chrysotile fibers revealed different efficiency depending on the fungi genus. Fungi such as *Fusarium oxysporum* released also in the extracellular medium chelators able to extract iron from both serpentine (chrysotile) and amphibole (amosite and crocidolite) asbestos fibers

[42]. Asbestos seems to be an iron source for various organisms described so far through the siderophore strategy.

1.3. Evidence of biofilm formation on asbestos fibers

In the experiment of iron dissolution by siderophore-producing bacteria, we observed that all raw asbestos incubated with bacteria were agglomerated, leading to a compact cluster, whereas the fibers resulting from deterioration in the abiotic medium remained free. In order to determine the impact of biotic condition on the material, fibers were observed by TEM (Fig. 3). As an example, crocidolite fibers incubated with *Pseudomonas aeruginosa* wild type or in the succinate medium after 48 h were analyzed. The analysis of the alterated fibers in abiotic conditions showed no detectable alteration layer. In biotic condition, fibers are covered with a biofilm explaining the agglomeration of the material. *Pseudomonas* are well known to form biofilm, which is a surface-attached bacteria embedded in a self-produced matrix of extracellular polymeric substances (EPS) that are adherent to each other and/or a surface exopolysaccharides (Fig. 3). Adhesion to surfaces has been seen as a survival strategy under energy limitation [44]. Weathering of rocks is a complex process where biofilm are able to accelerate or inhibit the alteration [45]. For example, *Pseudomonas aeruginosa* has already been described to form a biofilm on municipal waste incinerator bottom ash cementing grains together [46] or on smectite, a type of clay [31]. In leachates experiments of bottom ashes, analysis of iron concentration in solution increase in the presence of bacteria and bottom ash, while the concentration of others elements such as Ni and Zn was higher in abiotic condition compared to the biotic medium. This could be a consequence of chemical modification of the solution by bacterial development since reducing conditions together with the production of organic acids and siderophores may occur. Siderophore-promoted dissolution of iron-bearing minerals has been clearly documented and the study of Ferret *et al.* [31] showed an increase in the dissolved silicon, iron and aluminum concentrations following smectite supplementation in the presence of *Pseudomonas*. In an asbestos cement pipe in drinking water distribution system, a biofilm was evidenced containing metallic cations leading to decrease of the thickness of the pipe wall linked to the loss of hydrated cement matrix. A consequence of this bacterial activity may cause a pipe failure [47]. In our experiments, the analysis of crocidolite fibers by STEM-EDX showed a slight decrease of iron content after 48 h with bacterial contact. According to results in figure 2, the bacterial supernatant of the wild type *P. aeruginosa* allowed to deplete iron

more efficiently from fibers compared to bacterial cells. These results confirmed the active dissolution driven by the siderophore-mediated and/or bacterial process (Fig. 4).

4. Conclusions

We examined the potential bioweathering ability of siderophore-producing *Pseudomonas* and their produced siderophores on raw asbestos fibers. We clearly showed that biological chelating agents are more efficient in iron extraction than the best known chemical chelating compound EDTA. In addition, iron dissolution was more effective when fibers were manually grinded. Our results demonstrated that *Pseudomonas* and their produced siderophores, pyoverdine and pyochelin, were able to dissolve iron from asbestos fibers but not at the same efficiency. Siderophores containing supernatants extracted more iron than the bacterial cells after asbestos contact. A biofilm covering fibers was evidenced during bacterial growth and the iron content in fibers decreased after bacterial contact. Moreover, pyoverdine containing supernatant dissolved more rapidly iron from chrysotile and crocidolite fibers than pyochelin containing supernatant. Our study clearly demonstrated that either siderophores or *Pseudomonas* cells were able to weather the three types of asbestos fibers. Our research has shown that asbestos can serve as a source of nutrients for soil bacteria. Further investigations are required to extend these experiments on asbestos wastes in order to develop a bioremediation process based on bacterial and/or siderophore alteration.

Acknowledgements

This work was supported by the French Environment and Energy Management Agency (ADEME) and the SOMEZ (Société Méditerranéenne des Zéolithes).

References

[1] W.B. Simmons, Amphibole, Encyclopædia Britannica, Inc. (2016). https://www.britannica.com/science/amphibole.

[2] D. Bernstein, J. Dunnigan, T. Hesterberg, R. Brown, J.A.L. Velasco, R. Barrera, J. Hoskins, A. Gibbs, Health risk of chrysotile revisited, Crit Rev Toxicol. 43 (2013) 154–183. doi:10.3109/10408444.2012.756454.

[3] S. Toyokuni, Mechanisms of asbestos-induced carcinogenesis, Nagoya Journal of Medical Science. 71 (2009) 1–10.

[4] **M. Valko, K. Jomova, C.J. Rhodes, K. Kuča, K. Musílek, Redox- and non-redox-metal-induced formation of free radicals and their role in human disease, Arch Toxicol. 90 (2015) 1–37. doi:10.1007/s00204-015-1579-5.**

[5] **S.M. Kraemer, Iron oxide dissolution and solubility in the presence of siderophores, Aquat. Sci. 66 (2004) 3–18. doi:10.1007/s00027-003-0690-5.**

[6] **F. Watteau, J. Berthelin, Microbial dissolution of iron and aluminium from soil minerals: efficiency and specificity of hydroxamate siderophores compared to alphatic acids, European Journal of Soil Biology. 30 (1994) 1–9.**

[7] **S. Hiradate, K. Inoue, Dissolution of iron from iron (Hydr)Oxides by mugineic acid, Soil Science and Plant Nutrition. 44 (1998) 305–313. doi:10.1080/00380768.1998.10414453.**

[8] **B.E. Kalinowski, L.J. Liermann, S. Givens, S.L. Brantley, Rates of bacteria-promoted solubilization of Fe from minerals: a review of problems and approaches, Chemical Geology. 169 (2000) 357–370. doi:10.1016/S0009-2541(00)00214-X.**

[9] **D.R. Rosenberg, P.A. Maurice, Siderophore adsorption to and dissolution of kaolinite at pH 3 to 7 and 22°C, Geochimica et Cosmochimica Acta. 67 (2003) 223–229. doi:10.1016/S0016-7037(02)01082-7.**

[10] **M. Yao, B. Lian, H.H. Teng, Y. Tian, X. Yang, Serpentine Dissolution in the Presence of Bacteria Bacillus mucilaginosus, Geomicrobiology Journal. 30 (2013) 72–80. doi:10.1080/01490451.2011.653087.**

[11] **S. Bhattacharya, P.J. John, L. Ledwani, Bacterial Weathering of Asbestos, Silicon. 7 (2015) 419–431. doi:10.1007/s12633-014-9260-9.**

[12] **S. Bhattacharya, P.J. John, L. Ledwani, Fungal weathering of asbestos in semi arid regions of India, Ecotoxicology and Environmental Safety. 124 (2016) 186–192. doi:10.1016/j.ecoenv.2015.10.022.**

[13] **M. Rajkumar, N. Ae, M.N.V. Prasad, H. Freitas, Potential of siderophore-producing bacteria for improving heavy metal phytoextraction, Trends in Biotechnology. 28 (2010) 142–149. doi:10.1016/j.tibtech.2009.12.002.**

[14] **L.G. Lund, A.E. Aust, Iron mobilization from asbestos by chelators and ascorbic acid, Archives of Biochemistry and Biophysics. 278 (1990) 60–64. doi:10.1016/0003-9861(90)90231-M.**

[15] **C.C. Chao, A.E. Aust, Effect of Long-Term Removal of Iron from Asbestos by Desferrioxamine B on Subsequent Mobilization by Other Chelators and Induction of DNA Single-Strand Breaks, Archives of Biochemistry and Biophysics. 308 (1994) 64–69. doi:10.1006/abbi.1994.1009.**

[16] **C. Cocozza, G.L. Ercolani, Siderophore production and associated characteristics in rhizosphere and non-rhizosphere fluorescent pseudomonads, Annali di microbiol. enzimol. 47 (1997) 17–28.**

[17] **L. Hersman, T. Lloyd, G. Sposito, Siderophore-promoted dissolution of hematite, Geochimica et Cosmochimica Acta. 59 (1995) 3327–3330. doi:10.1016/0016-7037(95)00221-K.**

[18] **J.B. Goldberg, Pseudomonas: global bacteria, Trends Microbiol. 8 (2000) 55–57.**

[19] **K. Poole, G.A. McKay, Iron acquisition and its control in Pseudomonas aeruginosa: many roads lead to Rome, Front. Biosci. 8 (2003) d661-686.**

[20] **J.M. Meyer, M.A. Abdallah, The Fluorescent Pigment of Pseudomonas fluorescens: Biosynthesis, Purification and Physicochemical Properties, Microbiology. 107 (1978) 319–328. doi:10.1099/00221287-107-2-319.**

[21] **C.D. Cox, K.L. Rinehart, M.L. Moore, J.C. Cook, Pyochelin: novel structure of an iron-chelating growth promoter for Pseudomonas aeruginosa, PNAS. 78 (1981) 4256–4260. doi:10.1073/pnas.78.7.4256.**

[22] H. Budzikiewicz, Siderophores of Fluorescent Pseudomonads, Z. Naturforschung C. 52 (1997) 713–720. doi:10.1515/znc-1997-11-1201.

[23] H. Budzikiewicz, M. Schäfer, D.U. Fernández, S. Matthijs, P. Cornelis, Characterization of the chromophores of pyoverdins and related siderophores by electrospray tandem mass spectrometry, Biometals. 20 (2007) 135–144. doi:10.1007/s10534-006-9021-3.

[24] H. Budzikiewicz, Siderophores of the Pseudomonadaceae sensu stricto(Fluorescent and Non-Fluorescent Pseudomonas spp.), in: H. Budzikiewicz, T. Flessner, R. Jautelat, U. Scholz, E. Winterfeldt, W. Herz, H. Falk, G.W. Kirby (Eds.), Progress in the Chemistry of Organic Natural Products, Springer Vienna, Vienna, 2004: pp. 81–237. doi:10.1007/978-3-7091-0581-8_2.

[25] P. Demange, S. Wendenbaum, C. Linget, C. Mertz, M.T. Cung, A. Dell, M.A. Abdallah, Bacterial siderophores : structure and NMR assignment of pyoverdins Pa, siderophores ofPseudomonas aeruginosa ATCC 15692, Biol Metals. 3 (1990) 155–170. doi:10.1007/BF01140574.

[26] R. Fuchs, H. Budzikiewicz, Structural Studies of Pyoverdins by Mass Spectrometry, Curr. Org. Chem. 5 (2001) 265–288. doi:https://doi.org/10.2174/1385272013375562.

[27] A.-M. Albrecht-Gary, S. Blanc, N. Rochel, A.Z. Ocaktan, M.A. Abdallah, Bacterial Iron Transport: Coordination Properties of Pyoverdin PaA, a Peptidic Siderophore of Pseudomonas aeruginosa, Inorg. Chem. 33 (1994) 6391–6402. doi:10.1021/ic00104a059.

[28] J. Brandel, N. Humbert, M. Elhabiri, I.J. Schalk, G.L.A. Mislin, A.-M. Albrecht-Gary, Pyochelin, a siderophore of Pseudomonas aeruginosa: Physicochemical characterization of the iron(III), copper(II) and zinc(II) complexes, Dalton Trans. 41 (2012) 2820–2834. doi:10.1039/C1DT11804H.

[29] C.-F. Tseng, A. Burger, G.L.A. Mislin, I.J. Schalk, S.S.-F. Yu, S.I. Chan, M.A. Abdallah, Bacterial siderophores: the solution stoichiometry and coordination of the Fe(III) complexes of pyochelin and related compounds, J Biol Inorg Chem. 11 (2006) 419–432. doi:10.1007/s00775-006-0088-7.

[30] L.E. Hersman, J.H. Forsythe, L.O. Ticknor, P.A. Maurice, Growth of Pseudomonas mendocina on Fe(III) (Hydr)Oxides, Appl. Environ. Microbiol. 67 (2001) 4448–4453. doi:10.1128/AEM.67.10.4448-4453.2001.

[31] C. Ferret, T. Sterckeman, J.-Y. Cornu, S. Gangloff, I.J. Schalk, V.A. Geoffroy, Siderophore-promoted dissolution of smectite by fluorescent Pseudomonas, Environmental Microbiology Reports. 6 (2014) 459–467. doi:10.1111/1758-2229.12146.

[32] C. Reimmann, L. Serino, M. Beyeler, D. Haa, Dihydroaeruginoic acid synthetase and pyochelin synthetase, products of the pchEF, are induced by extracellular pyochelin in Pseudornonas aeruginosa, Microbiology. 144 (1998) 3135–3148. doi:10.1099/00221287-144-11-3135.

[33] F. Hoegy, X. Lee, S. Noel, D. Rognan, G.L.A. Mislin, C. Reimmann, I.J. Schalk, Stereospecificity of the Siderophore Pyochelin Outer Membrane Transporters in Fluorescent Pseudomonads, J. Biol. Chem. 284 (2009) 14949–14957. doi:10.1074/jbc.M900606200.

[34] B. Nowack, F.G. Kari, H.G. Krüger, The Remobilization of Metals from Iron Oxides and Sediments by Metal-EDTA Complexes, Water, Air, & Soil Pollution. 125 (2001) 243–257. doi:10.1023/A:1005296312509.

[35] D. Spasiano, F. Pirozzi, Treatments of asbestos containing wastes, Journal of Environmental Management. 204, Part 1 (2017) 82–91. doi:10.1016/j.jenvman.2017.08.038.

[36] A.J. Werner, M.F. Hochella, G.D. Guthrie, J.A. Hardy, A.E. Aust, Rimstidt, Asbestiform riebeckite (crocidolite) dissolution in the presence of Fe chelators: Implications for mineral-induced disease, American Mineralogist. 80 (2015) 1093–1103. doi:10.2138/am-1995-11-1201.

[37] S.K. Mohanty, C. Gonneau, A. Salamatipour, R.A. Pietrofesa, B. Casper, M. Christofidou-Solomidou, J.K. Willenbring, Siderophore-mediated iron removal from chrysotile: Implications for asbestos toxicity reduction and bioremediation, Journal of Hazardous Materials. 341 (2018) 290–296. doi:10.1016/j.jhazmat.2017.07.033.

[38] R.L. Virta, Asbestos: geology, mineralogy, mining, and uses, US Department of the Interior. US Geological Survey, 2002. http://pubs. usgs. gov/of/2002/of02-149/index. html (accessed November 16, 2016).

[39] E. Ahmed, S.J.M. Holmström, Siderophores in environmental research: roles and applications, Microbial Biotechnology. 7 (2014) 196–208. doi:10.1111/1751-7915.12117.

[40] P. Plescia, D. Gizzi, S. Benedetti, L. Camilucci, C. Fanizza, P. De Simone, F. Paglietti, Mechanochemical treatment to recycling asbestos-containing waste, Waste Management. 23 (2003) 209–218. doi:10.1016/S0956-053X(02)00156-3.

[41] A. Salamatipour, S.K. Mohanty, R.A. Pietrofesa, D.R. Vann, M. Christofidou-Solomidou, J.K. Willenbring, Asbestos Fiber Preparation Methods Affect Fiber Toxicity, Environ. Sci. Technol. Lett. 3 (2016) 270–274. doi:10.1021/acs.estlett.6b00174.

[42] S. Daghino, E. Martino, I. Fenoglio, M. Tomatis, S. Perotto, B. Fubini, Inorganic Materials and Living Organisms: Surface Modifications and Fungal Responses to Various Asbestos Forms, Chem. Eur. J. 11 (2005) 5611–5618. doi:10.1002/chem.200500046.

[43] S. Daghino, E. Martino, E. Vurro, M. Tomatis, M. Girlanda, B. Fubini, S. Perotto, Bioweathering of chrysotile by fungi isolated in ophiolitic sites, FEMS Microbiology Letters. 285 (2008) 242–249. doi:10.1111/j.1574-6968.2008.01239.x.

[44] K.C. Marshall, Mechanisms of Bacterial Adhesion at Solid-Water Interfaces, in: D.C. Savage, M. Fletcher (Eds.), Bacterial Adhesion: Mechanisms and Physiological Significance, Springer US, Boston, MA, 1985: pp. 133–161. doi:10.1007/978-1-4615-6514-7_6.

[45] D. Mottershead, A. Gorbushina, G. Lucas, J. Wright, The influence of marine salts, aspect and microbes in the weathering of sandstone in two historic structures, Building and Environment. 38 (2003) 1193–1204. doi:10.1016/S0360-1323(03)00071-4.

[46] G. Aouad, J.-L. Crovisier, D. Damidot, P. Stille, E. Hutchens, J. Mutterer, J.-M. Meyer, V.A. Geoffroy, Interactions between municipal solid waste incinerator bottom ash and bacteria (Pseudomonas aeruginosa), Science of The Total Environment. 393 (2008) 385–393. doi:10.1016/j.scitotenv.2008.01.017.

[47] D. Wang, R. Cullimore, Y. Hu, R. Chowdhury, Biodeterioration of asbestos cement (AC) pipe in drinking water distribution systems, International Biodeterioration & Biodegradation. 65 (2011) 810–817. doi:10.1016/j.ibiod.2011.05.004.

FIGURE LEGENDS:

Figure 1: Iron concentration dissolved from raw asbestos grinded or not in the presence of EDTA (200 µM) (grey bars) or purified pyoverdine (200 µM) from *Pseudomonas aeruginosa* ATCC 15692 (black bars) after two 48 hours-contact time and a 96 hours contact time under shaking (200 rpm) at 30°C. Iron was monitored by atomic absorption spectroscopy in the absence or in the presence of asbestos (0.125 g). Raw asbestos were designed as chrysotile (CHR) or grinded chrysotile (CHRb), crocidolite (CRO) or grinded crocidolite (CROb), amosite (AMO) or grinded amosite (AMOb). Error bars indicates standard deviation over mean of triplicate experiments. Groups without significant different iron amounts were indicated by a, b, and c.

Figure 2: Iron concentration measured in the supernatant after bacterial growth (B,D, F) or in the presence of each bacterial strain's supernatant (A, C, E) after 3 renewal cycles of 48 H with raw chrysotile (A, B), raw crocidolite (C, D) and raw amosite (E, F) at 30°C. The tested strains were the wild-type *Pseudomonas aeruginosa* ATCC 15691 (PAO1, red bars), pyocheline-deficient mutant (□PCH, green bars) and pyoverdine-deficient mutant (□PVD, blue bars). Error bars indicates standard deviation over mean of triplicate experiments.

Figure 3: STEM images of bacterial biofilm associated to crocidolite fibers (B) compared to control fibers (A). Crocidolite fibers were incubated with the wild-type *Pseudomonas aeruginosa* in succinate medium or succinate medium without bacteria during 48 h under shaking condition (220 rpm). Scale bar corresponds to 500 nm.

Figure 4: STEM images and STEM mappings of crocidolite fibers before contact (a and b), after bacterial growth (c and d) and after incubation with bacterial supernatant (e and f) during 48 h under shaking conditions (220 rpm). Large images obtained from the combination of the three distributions of Mg, Si, and Fe with analysis areas (a, c and e). Atomic ratios of Mg/Si and Fe/Si (b, d and f). Mass percentage of iron, magnesium and silicium before and after contact of raw crocidolite with *P. aeruginosa* PAO1 or bacterial supernatant (g).

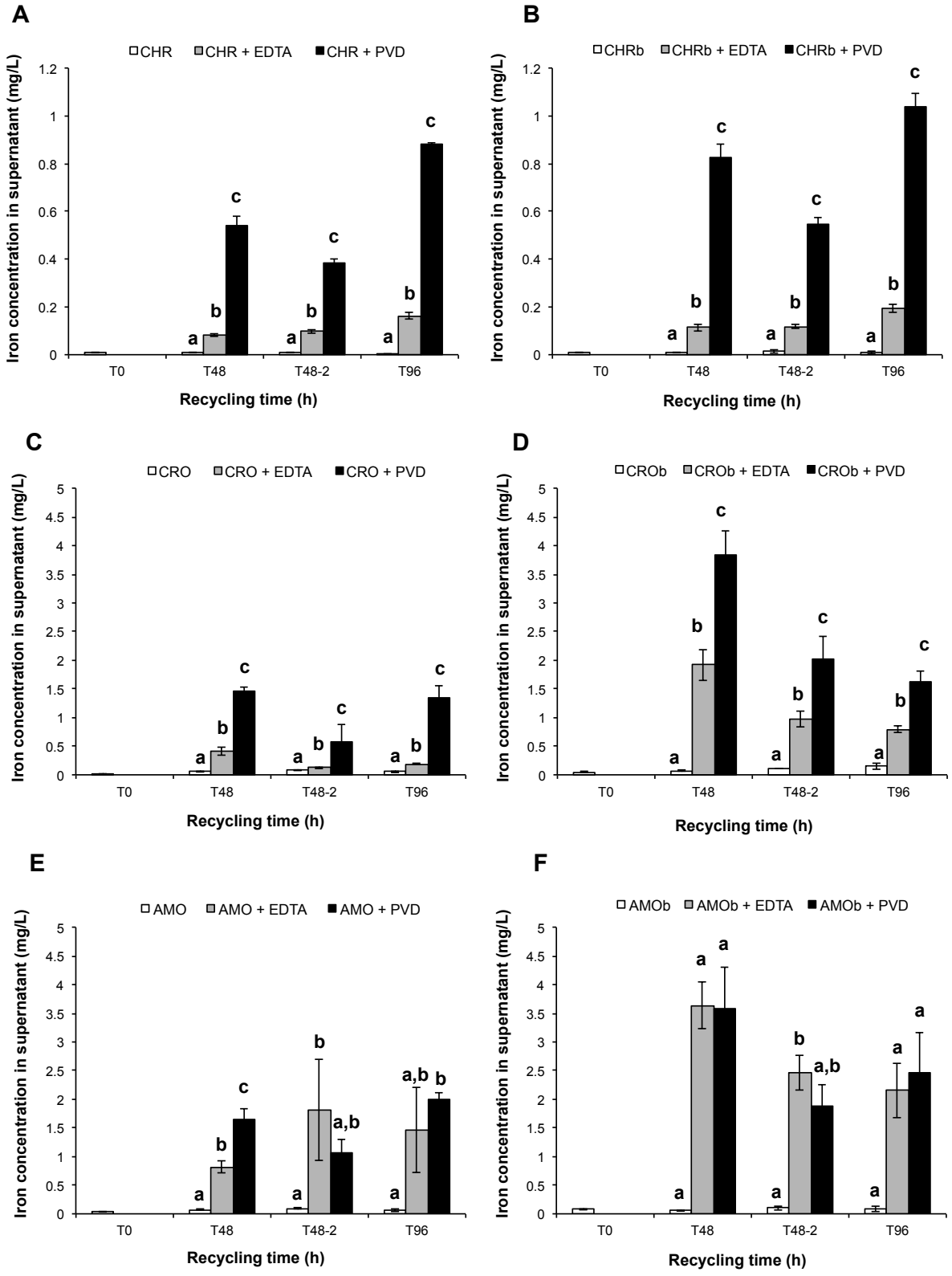

Figure 1: Iron concentration dissolved from raw asbestos grinded or not in the presence of EDTA (200 µM) (grey bars) or purified pyoverdine (200 µM) from *Pseudomonas*

aeruginosa ATCC 15692 (black bars) after two 48 hours-contact time and a 96 hours contact time under shaking (200 rpm) at 30°C. Iron was monitored by atomic absorption spectroscopy in the absence or in the presence of asbestos (0.125 g). Raw asbestos were designed as chrysotile (CHR) or grinded chrysotile (CHRb), crocidolite (CRO) or grinded crocidolite (CROb), amosite (AMO) or grinded amosite (AMOb). Error bars indicates standard deviation over mean of triplicate experiments. Groups without significant different iron amounts were indicated by a, b, and c.

1

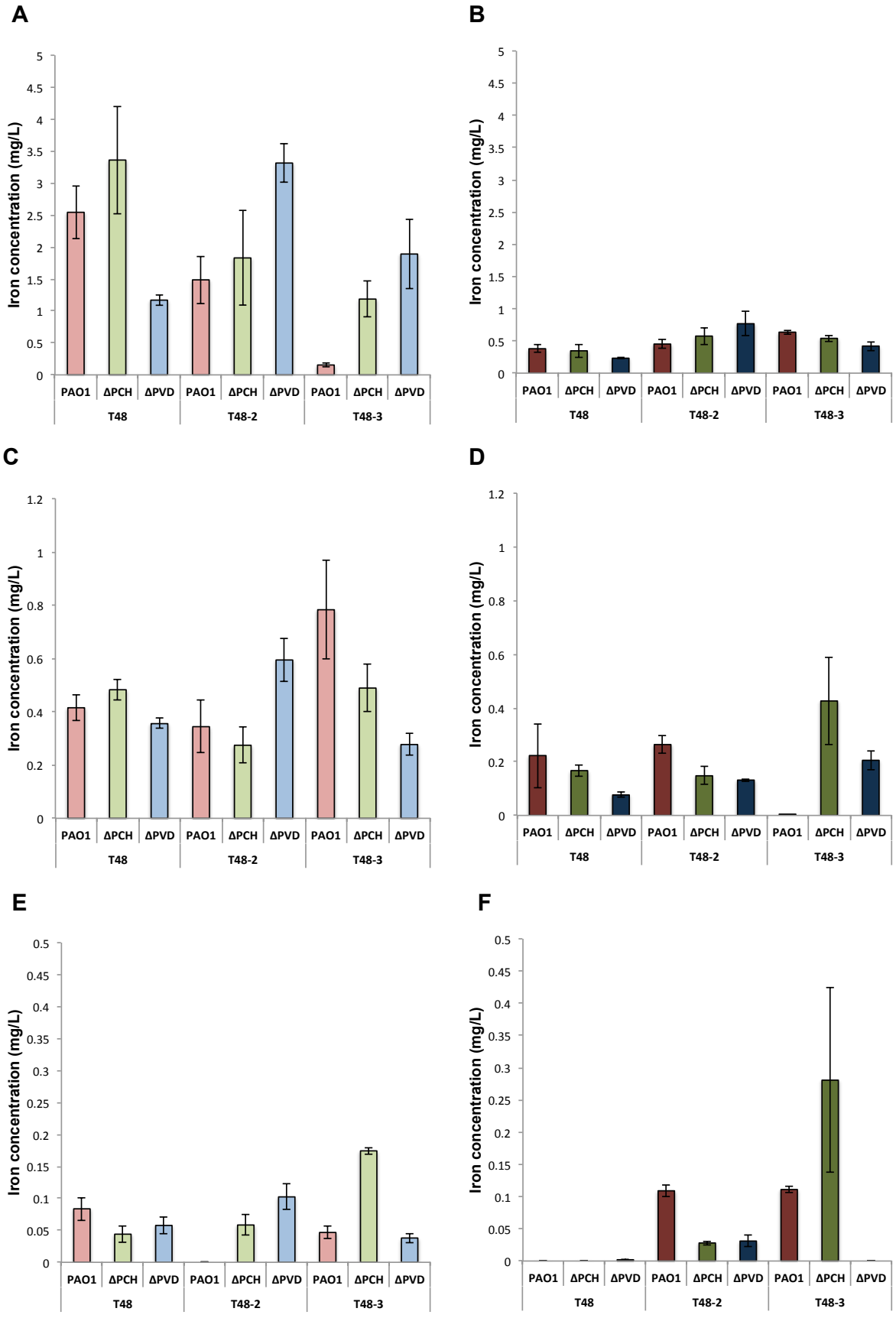

2
3
4

Figure 2: Iron concentration measured in the supernatant after bacterial growth (B,D, F) or in the presence of each bacterial strain's supernatant (A, C, E) after 3 renewal cycles of 48 H with raw chrysotile (A, B), raw crocidolite (C, D) and raw amosite (E, F) at 30°C. The tested strains were the wild-type *Pseudomonas aeruginosa* ATCC 15691 (PAO1, red bars), pyochelin-deficient mutant (ΔPCH, green bars) and pyoverdine-deficient mutant (ΔPVD, blue bars). Error bars indicates standard deviation over mean of triplicate experiments.

In color print

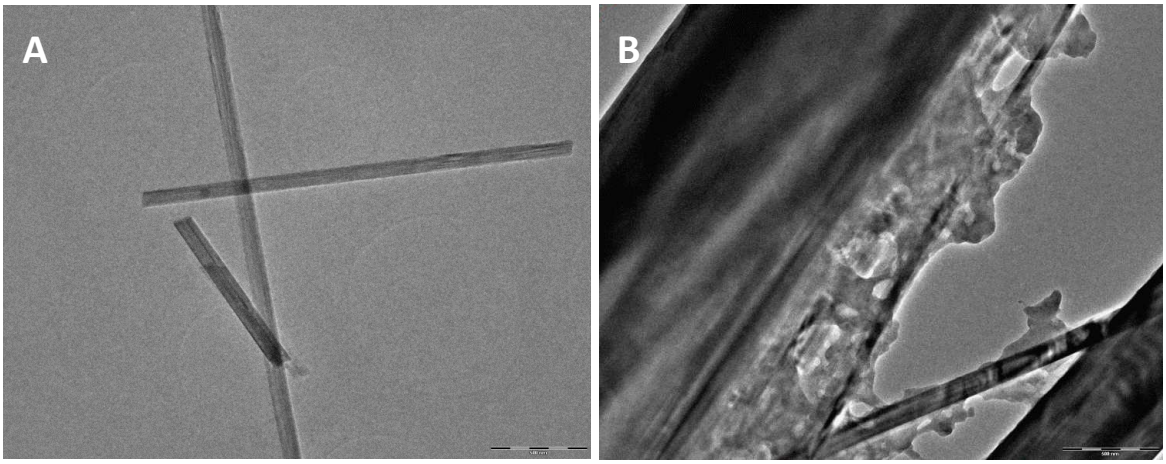

Figure 3: STEM images of bacterial biofilm associated to crocidolite fibers (B) compared to control fibers (A). Crocidolite fibers were incubated with the wild-type *Pseudomonas aeruginosa* in succinate medium or succinate medium without bacteria during 48 h under shaking condition (220 rpm). Scale bar corresponds to 500 nm.

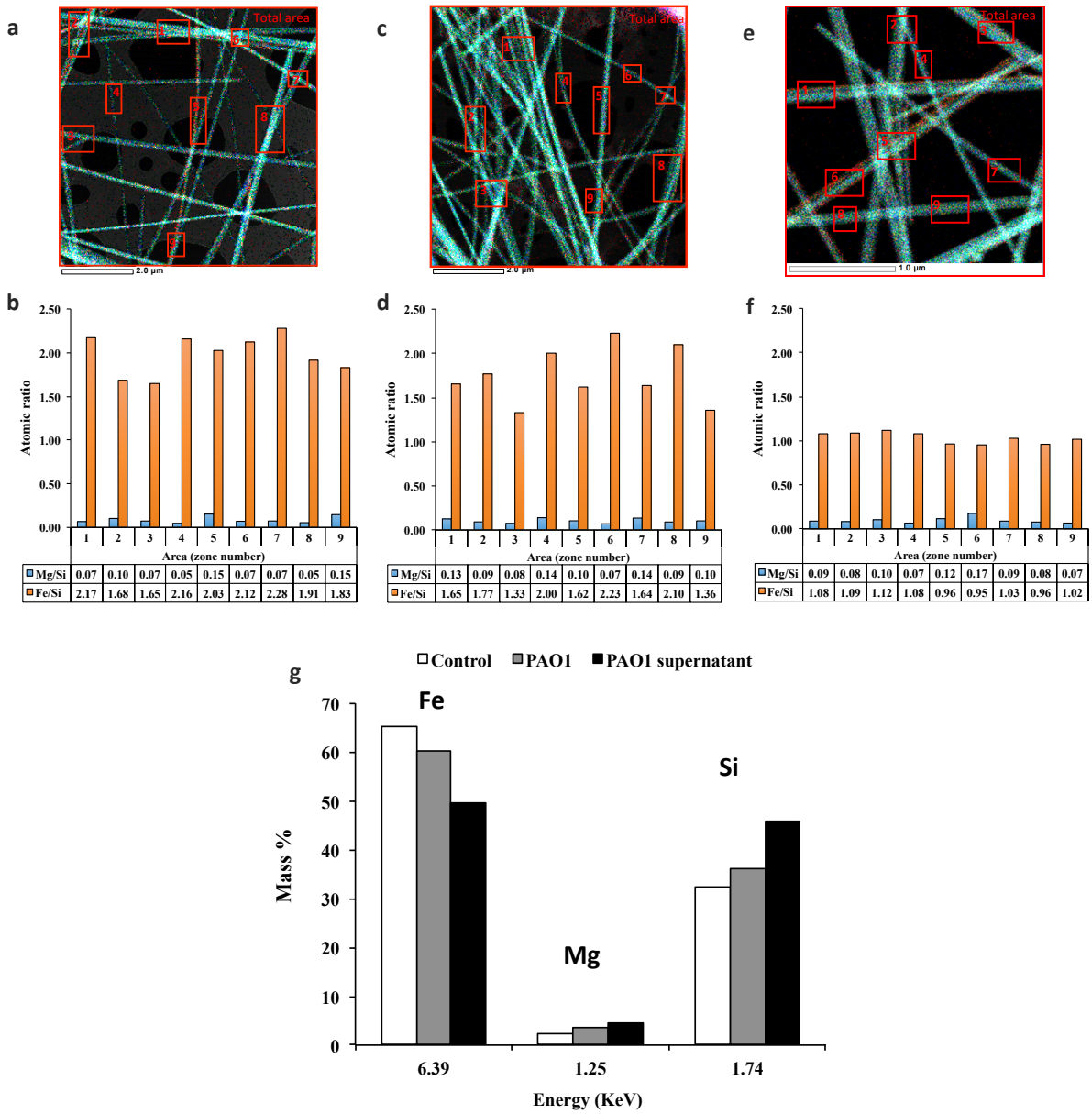

Figure 4: STEM images and STEM mappings of crocidolite fibers before contact (a and b), after bacterial growth (c and d) and after incubation with bacterial supernatant (e and f) during 48 h under shaking conditions (220 rpm). Large images obtained from the combination of the three distributions of Mg, Si, and Fe with analysis areas (a, c and e). Atomic ratios of Mg/Si and Fe/Si (b, d and f). Mass percentage of iron, magnesium and silicium before and after contact of raw crocidolite with *P. aeruginosa* PAO1 or bacterial supernatant (g)

In color print

Table 1. List and composition of asbestos used.

Name	Composition	Source
Chrysotile	$Mg_6Si_4O_{10}(OH)_8$	Natural History Museum of Paris
Crocidolite	$Na_2(Fe^{3+})_2(Fe^{2+})_3Si_8O_{22}(OH)_2$	mine South Africa « Wangu Hill, Kwagulu, province of Natal Woumo
Amosite	$(Fe, Mg)_7Si_8O_{22}(OH)_2$	Penga mine- South Africa, province of Impopo

Table 2. List of the strains used.

Name	Relevant characteristics	Reference or source
***P. aeruginosa* strains**		
PAO1	Wild-type	ATCC15692
PAO6297	Δ*pchBA*	[32]
PAO6382	ΔpvdF	[33]

Graphical Abstract